Journal of Mines, Metals and Fuels, *72(2): 179-187; 2024. DOI: 10.18311/jmmf/2024/35988*

Print ISSN : 0022-2755

Journal of Mines, Metals and Fuels

Contents available at: *www.informaticsjournals.com/index.php/jmmf*

Effect of Reinforcement on Micro Structural and Compressive Deformation Behavior on Closed Cell AA7075 Aluminium Foam

Nitish Kumar Singh[1]*, S. Balaguru[2], Pavan Mehta[3], Amit Kaimkuriya[4], Avinash Kumar Namdeo[1] and Rupak Kumar Deb[1]

[1]Department of Mechanical Engineering, Lingaya's Vidyapeeth, Faridabad - 121002, Haryana, India; hknitish@gmail.com

[2]School of Mechanical Engineering, VIT Bhopal University, Sehore - 466114, Madhya Pradesh, India

[3]Department of Electrical Engineering, Medi-Caps University, Indore - 453331, Madhya Pradesh, India

[4]Department of Mechanical Engineering, Mittal Institute of Technology, Bhopal - 462038, Madhya Pradesh, India

Abstract

The fabrication of aluminium AA7075 and AA7075/SiC composite foams employ the stir casting method, incorporating calcium carbonate ($CaCO_3$) as a blowing agent at a concentration constituting 2.5wt. % of the alloy. Notably, no viscosity-enhancing component was included in the process. The compressive parameters, including the yield strength (σc), plateau stress (σpl) and energy absorption (Eab), of the foam materials were examined to investigate the influence of Silicon Carbide (SiC) on the microstructure, namely the cell size and cell wall thickness. The incorporation of Silicon Carbide particles (SiC) into the cell wall imparts enhanced hardness and strength. The findings indicate that the inclusion of SiC particles may enhance the mechanical properties like σc, σp and Eab, of composite foams. The porosity of the composite foam increases from 59.07% to 68.68% with the incorporation of SiC particles. The cell dimensions fluctuated between 1.12 and 1.45mm as the relative density of the AA7075/SiC composite foam decreased from 0.4 to 0.31.

Keywords: *AA7075, Cell Wall, Energy Absorption, Plateau Stress, Silicon Carbide*

1.0 Introduction

Aluminium and alloy foams have garnered significant attention in recent times owing to their very low density, unique functional characteristics and capacity to facilitate energy absorption, sound absorption and flame resistance[1,2]. The 'Cell' word comes from the Latin word 'cella' which means a small section having an enclosed vacant space. Our attention is on packets of cells that are 'cellarium' for Romans but for us cellular solid is more familiar. According to this the assemblage of cells is the combination of solid faces, edges and space arrangement that is called porous materials. Such porous materials are very common in nature i.e. wood, bone, sponge, cork, etc. In numerous methods, aluminium metal can be incorporated into composites and foams. These include stir-casting methods[3-5], powder metallurgy[6], sintering method, liquid diffusion welding method[6], foaming compact blowing agents and building of gas in melt injection employing foaming agents. Metal foam is useful for the automotive and aviation industries because of a variety of mechanical and physical properties, including

**Author for correspondence*

its low weight, high explicit stiffness, outstanding strength-to-weight ratios and significantly improved energy absorption capacities[7-9]. The metal aluminium foam is regarded as a substance that is solid at low pressure but behaves like a liquid under high pressure[10-12]. The powder metallurgy method can also be used to make aluminium metal foams. It is done by heating a tightly packed mix of aluminium metal and a foaming agent[13]. The degraded TiH_2 emits hydrogen gas into the liquid compact of aluminium foam in the aluminium lattice. The PM foaming process is associated with rapid development which results in a usable cellular structure of foam in a matter of moments[14]. The stir casting method is a highly efficient manufacturing procedure used for the fabrication of aluminium metal composites and foams, yielding successful results in the examination of mechanical applications[14-16].

The researchers attempted to produce AA7075 (without reinforcement) and AA7075/SiC (with reinforcement) composite foam in this study. Calcium Carbonate ($CaCO_3$) was used as a foaming agent in the preparation of AA7075 (without reinforcement foam) and AA7075/SiC (with reinforcement) composite foam. This study aims to improve the mechanical properties and energy-absorbing capabilities of composite foams. AA7075 and AA7075/SiC composite foams are characterised as functions of density and the mechanical properties are compared to those of aluminium AA7075 foam.

2.0 Experimental Details

2.1 Materials

Typically, the utilisation of metal foams depends on various factors like the composition of the foam matrix, its density, the arrangement of its cells, and whether they have open or closed porosity. AA7075 stands out for its high mechanical strength and impressive corrosion resistance. In comparison to standard aluminium, it exhibits superior fatigue strength, resistance to creep and formability. Due to its exceptional heat resistance and low specific gravity, this alloy is frequently chosen as the base material for the matrix in various applications, finding relevance across diverse industries such as transportation, sports, aircraft and electronics (Rathore *et al.*, 2022). Tables 1 and 2 provide a comprehensive overview of the chemical compositions and mechanical properties of the AA7075 alloy and the AA7075/SiC composite used in this work.

Table 1. Matrix material's chemical composition

Element	Weight %	Atomic %
C	1.09	2.29
O	15.10	23.54
Mg	0.82	0.84
Al	70.17	64.93
Si	6.74	6.00
Ca	0.07	0.04
Fe	0.82	0.37
Cu	1.33	0.52
Zn	3.87	1.48

2.2 Material Synthesis

In this study, the melt foaming technique was employed to create two separate sets of closed-cell aluminium foam, adhering to the subsequent procedures. The first

Table 2. Properties of matrix material

Density	Melting Point	Modulus of Elasticity	Poisons Ratio	Specific Heat	Tensile Strength	Yield Strength
2.81 g/cm^3	635^{0}C	70-80 GPa	0.35	960 Kg-K	230 MPa	a

Figure 1. Calcium carbonate foaming agent (10±5 µm).

Figure 2. Molten metal in graphite crucible.

stage was the division of a composite ingot consisting of AA7075 and AA7075+7% SiC aluminium alloy into smaller pieces. Subsequently, these fragments underwent a thorough cleaning procedure using acetone. A graphite crucible is used to contain purified particles, also known as the charge. The AA7075 and AA7075+7% SiC alloys were subjected to a stir casting process in an electric arc furnace, where they were melted at a temperature of 800°C. A flux of 20 grams was then added to the molten alloy and stirred at 5 minutes to remove impurities and then the temperature was lowered to 750°C. A calcium carbonate ($CaCO_3$) sample with a weight percentage of 2.5% was subjected to heat treatment at a temperature of 200°C. The resulting particles had a size range of 10±5 µm, as seen in Figure 1. Two separate additions of this treated calcium carbonate were made and agitated for a duration of 10 minutes to ensure even dispersion of the powder. Following stirring, the molten substance is maintained

Table 3. Process parameter for stirring

Variables	Quantity
Temperature (^{0}C)	750
Stirring Speed (rpm)	450-500
Time (min)	5
Preheat Temp. of Foaming Agent (^{0}C)	200

at 730°C within the furnace (Figure 2) enabling the decomposition of $CaCO_3$ into carbon dioxide (CO_2) gas, resulting in the creation of foam. Ultimately, the compact foam is retrieved from the crucible and further foam samples are generated by a machining process to enable the analysis and evaluation of its properties.

2.3 Microstructure Evaluation

To reduce the cellular damage, the specimens were transformed into cylindrical shapes with dimensions of 20mm × 20mm × 20mm, as seen in Figure 3, using a wire EDM machine. Following that, the specimens were subjected to etching and polishing using a typical metallographic procedure, as seen in Figure 3. This method facilitated the examination using a ZEISS EVO 18 scanning electron microscope and Energy-Dispersive X-ray spectroscopy (EDX), Scanning Electron Microscopy (SEM) and EDX analyses were conducted to scrutinise the distribution of the reinforced material, specifically Silicon Carbide (SiC), within the foams. Furthermore, the objective of the research was to examine the integration of reinforcement and the overall level of bonding between the two specimens.

2.4 Compressive Testing

The compression testing of the material specimens was conducted using the TUE/C-400 Universal Testing Machine (UTM) as seen in Figure 5. The specimens used for compression testing were created with dimensions of 60mm * 60mm * 30mm using an EDM wire-cutting machine, as seen in Figures 6 and 7. The testing method was executed with the TUE-C 400 Universal Testing

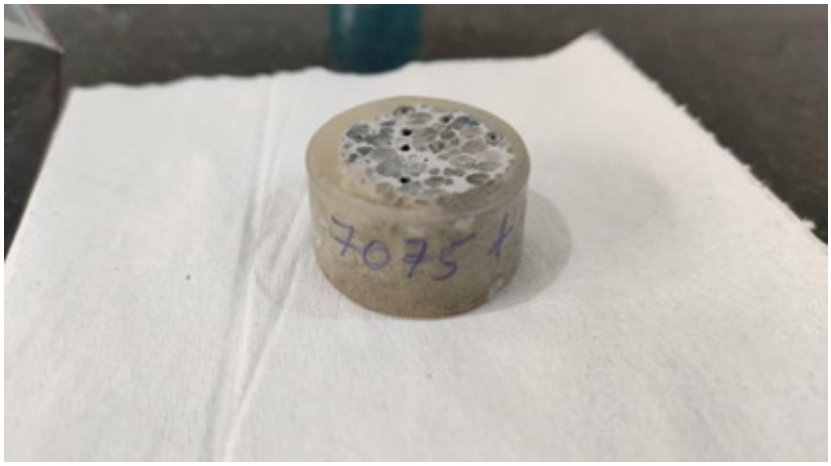

Figure 3. SEM testing specimen.

Figure 4. Setup (Scanning electron microscope).

Machine (UTM) which operated at a crosshead speed of 1mm/min and has a maximum load capacity of 400 kN. To evaluate the dependability of the observations, an analysis was conducted on three samples of each kind.

2.5 Energy Absorption

The amount of energy that metal foams take in when they are compressed is shown by the area under the stress-strain graph up to ε_D. The following equation was used to show the E_{ab} of aluminium foam:

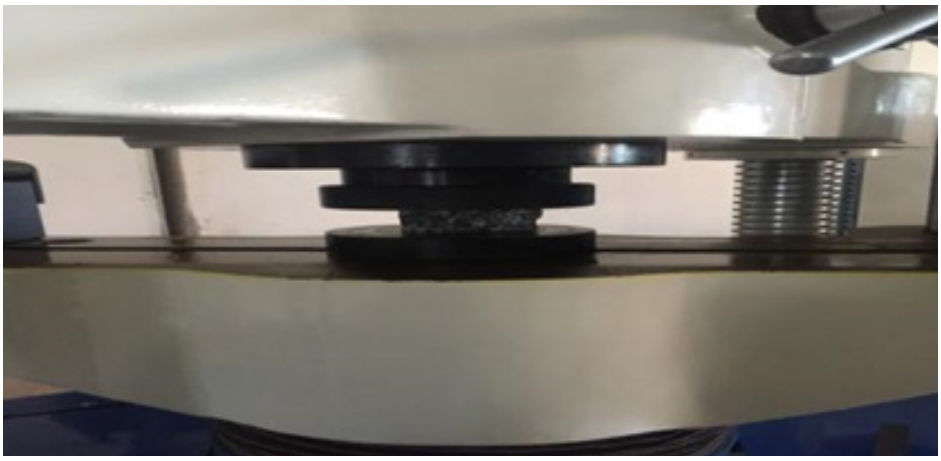

Figure 5. Loaded UTM machine.

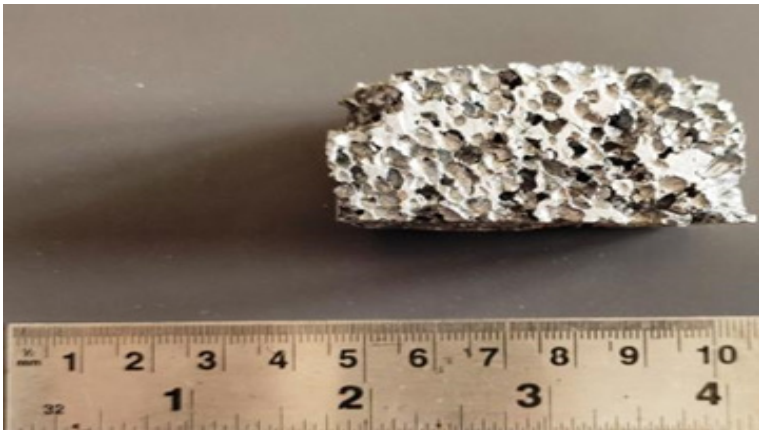

Figure 6. AA7075 foam.

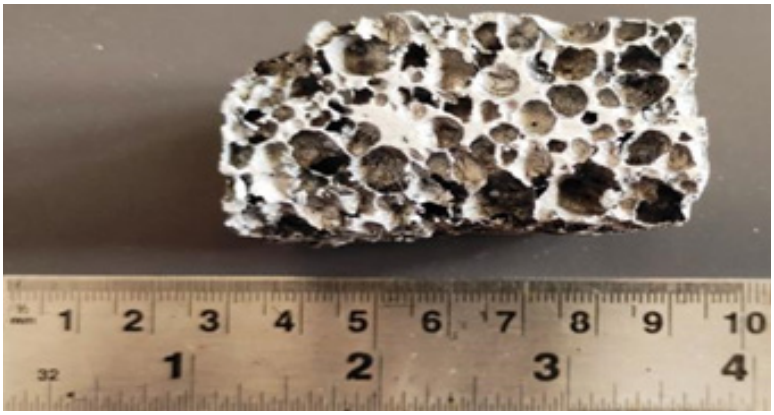

Figure 7. AA7075/SiC composite foam.

$$E_{ab} = \int_0^{\varepsilon_D} \sigma_{pl} \quad (1)$$

Where σ_{pl} and ε_D denote the plateau stress and densification strain, respectively. The energy absorption efficiency (ξ_{ab}) of aluminium foam was estimated using the following equation;

$$\xi_{ab} = \frac{E_{ab}}{(\sigma_{max} \cdot \varepsilon_D)} \times 1 \quad (2)$$

3.0 Results and Discussions

3.1 Micro-Structural Investigations

Figures 8 and 9 show the SEM spectra of both foam samples. The findings for both AA7075 and AA7075/SiC foam are shown in Table 4, which displays the outcomes obtained via the use of Image software for the analysis of cell size and cell wall thickness.

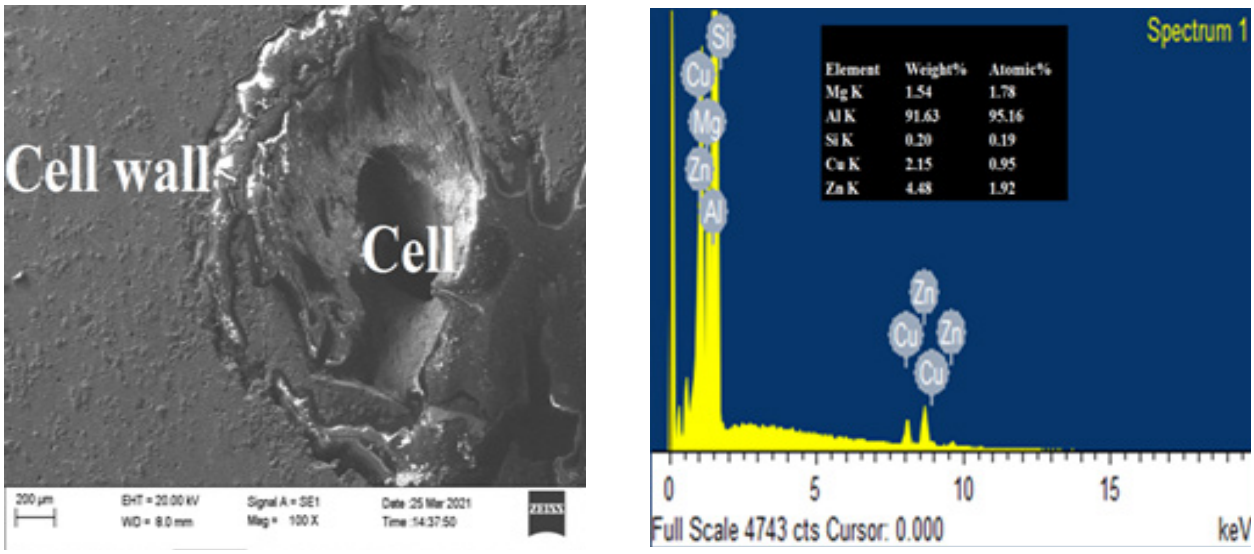

Figure 8. SEM and EDX spectrum of AA7075 composite.

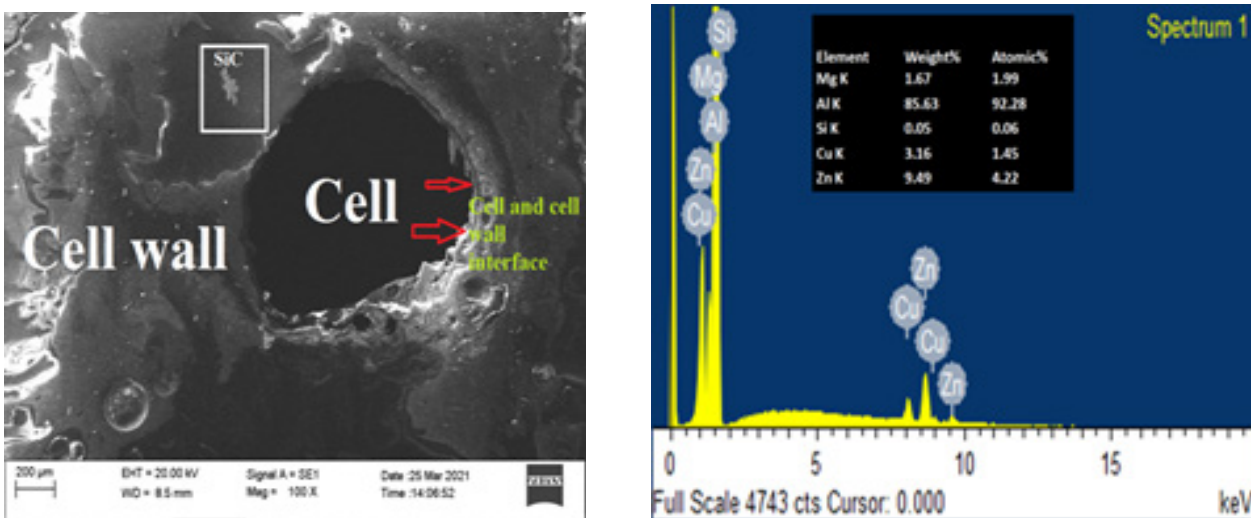

Figure 9. SEM and EDX spectrum of AA7075 composite spectrum of AA7075/SiC composite.

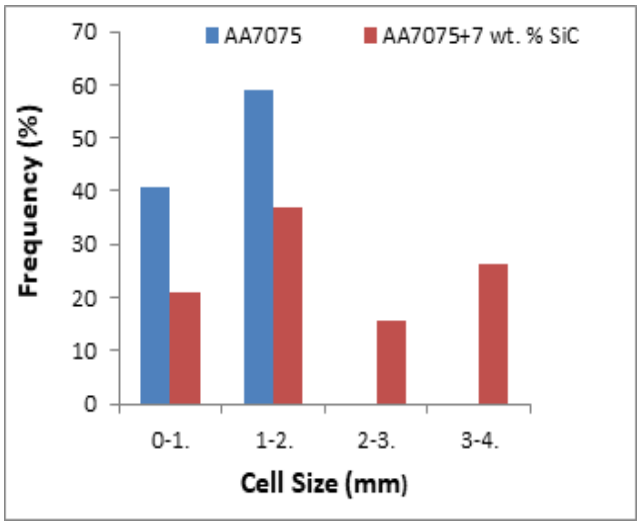

Figure 1. Cell size distribution.

From the microstructure analysis, it is clear that due to the addition of SiC particles, the pore size increases from 1.12 to 1.45 mm as well as the cell wall thickness reduces from 802.32 to 578 µm. Due to the viscosity in AA7075/SiC composite during the formation of foam being more than unreinforced composite, it seems that SiC contributes to inter-metallic and oxide phases such as $CaAl_2Si_2$, $CaAl_2Si_2O_8$, and SiO_2. This is clear evidence that SiC particle works as viscosity enhancing agent as well as a stabilising agent for closed cell structure. The addition of Reinforcement SiC particles plays a significant role in the relative density of fabricated foam. Due to the addition of SiC particles the relative density of reinforced composite foam reduces simultaneously. The porosity of the material increases because of the addition of SiC, particle viscosity of the melt increases and larger cell-size foam is produced which is shown in Figure 10.

3.2 Compression Deformation Behavior

Figure 11 depicts the compressive stress-strain curve accomplished from a quasi-static compression test performed on both foams. The stress-strain curve displays three distinct deformation regions within the AA7075 and AA7075/SiC composite foam:

(I) Linear Elastic Zone: In this phase, compressive stress changes proportionally with strain until it reaches the yield stress.

(II) As per ISO 13314 guidelines, the plateau stress refers to the mean stress value within the strain range of 0.2 to 0.4. This plateau zone demonstrates nearly constant compressive stress concerning strain.

(III) Densification Zone: This zone signifies the rapid increase in stress with a slight increase in strain, occurring when the cells within the foam structure are completely crushed.

Table 4. Physical properties of AA7075 and AA7075/ SiC composite foam

	Density (g/cm^3)	**Relative Density**	**Porosity %**	**Cell Size (mm)**	**Cell wall Thickness** (µm)
AA7075 Composite Foam	1.15	0.40	59.07	1.12	802.32
AA7075/SiC Composite Foam	0.88	0.31	68.68	1.45	578

Table 5. Physical properties of AA7075 and AA7075/SiC composite foam

	σ_c (MPa)	**σ_{pl} (MPa)**	**ε_D (mm/mm)**	**E_{ab} (MJ/m^3)**	**ξ_{ab} in %)**
AA7075	4.9	4.1	0.44	1.804	83.67
AA7075/ SiC	13.56	11.2	0.389	5.488	86.82

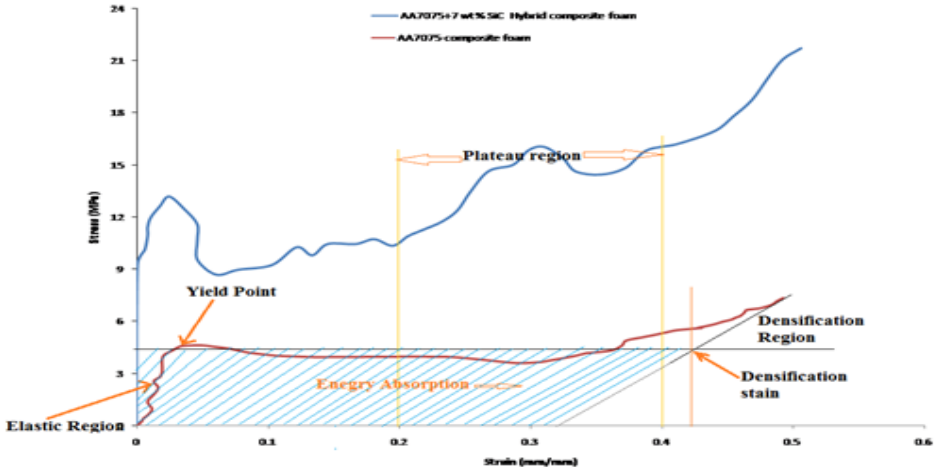

Figure 11. Stress-Strain curve.

The term "densification strain" (ε_D) refers to the stain value that is found at the intersection of the plateau line and the tangent line drawn at the point where the densification area has its maximum curvature. The yield stress (σ_c), plateau stress (σ_{pl}) and Densification stress (ε_D) are taken from the stress-strain curve for both the foams depicted in Table 5.

The yield stress and average plateau stress of the AA7075/SiC composite foam (SiC reinforced foam) were higher than those of the AA7075 foam (unreinforced composite foam), as shown in Table 5. The yield strength of AA7075/SiC composite foam (SiC reinforced composite foam) is about 3 times more than AA7075 foam. SiC-reinforced composite foam absorbs 67.12% more energy during static compression than unreinforced foam. Because of the SiC particle placed inside the cell wall and cell structure, as illustrated in Figures 8 and 9, which work as a binder, the compressive characteristics of AA7075/SiC (SiC reinforced foam) are superior (yield strength and average plateau strength) compared to unreinforced composite foam. The Densification strain (ε_D) of AA7075/SiC AHCFs (SiC reinforced) is slightly more when compared with AA7075 foam (unreinforced composite foam) due to which they follow the same deformation mechanism (layer-wise crushing).

4.0 Conclusion

The composite foam and the AA7075+SiC reinforced foam, with relative densities spanning from 0.40 to 0.31, were effectively manufactured through the melt route technique, specifically employing the Stir casting procedure. The procedure included the use of 2.5 weight per cent of $CaCO_3$ as the blowing agent, without the inclusion of viscosity additives. The subsequent point of emphasis lies in the observation that_

1. The average cell size of SiC-reinforced composites was found to be less than that of unreinforced composites because SiC-reinforced composite foam has a lower relative density. This indicates that SiC works as a thickening agent.
2. Energy Dispersive EDX at different spectrums conformed the uniform distribution of reinforcement in the AA7075/SiC composite foam.
3. Silicon carbide-reinforced composite foam exhibits superior yield strength and average plateau stress strength.
4. SiC-reinforced composite foam has a 67.12% higher energy absorption capacity during static compression than unreinforced composite foam

5.0 References

1. Rathore RK, Singh NK, Sinha AK, Panthi K, Sharma AK. Mechanical properties of lightweight Aluminium Hybrid Composite Foams (AHCFs) for structural applications. Adv Mater Process

Technol [Internet]. 2022; 8(2):1-15. Available from: https://doi.org/10.1080/2374068X.2022.2048498
2. Singh NK, Balaguru S. Experimental analysis of foaming agent contents in AA7075/SiC closed cell aluminium composite foam. In: Sethuraman B, Jain P, Gupta M, editors. Recent Advances in Mechanical Engineering. Singapore: Springer Nature Singapore; 2023; 567-75. https://doi.org/10.1007/978-981-99-2349-6_51
3 Rathore RK, Singh NK, Xavier JF. Characterisation of AA7075 alloy foam using calcium and magnesium carbonate as foaming agents. In 2021; 289-97. Available from: https://doi.org/10.1007/978-981-16-3937-1_30
4. Sowmiya S, Nallanukala P, Anburaj J, Simhachalam B. Development of metallic aluminium foam casting using calcium carbonate precursors for side impact beam application. Mater Today Proc [Internet]. 2018; 5(9):20362-70. https://doi.org/10.1016/j.matpr.2018.06.411
5. Osman HOA, Omran AM, Atlam AA, Kh MM. Fabrication of aluminium foam from aluminium scrap. Hamza. Int J Eng Res Appl. 2015; 5(2):109-15.
6. Kennedy AR, Asavavisitchai S. Effects of TiB2 particle addition on the expansion, structure and mechanical properties of PM Al foams. Scr Mater. 2004; 50(1):115-9. https://doi.org/10.1016/j.scriptamat.2003.09.026
7. Aravind AP, Kurmi JS, Swamy PM, Kumar SR, Rajak S, Kannan TDB. Optimisation of welding parameters in laser welding of Ti6Al4V using VIKOR optimisation method q. Mater Today Proc [Internet]. 2021; 45:592-6. Available from: https://doi.org/10.1016/j.matpr.2020.02.388
8. Kumar N, Balaguru SS. Fabrication and mechanical characterisation of Al Zn Cu Alloy / SiC/TiB2 hybrid reinforced metal matrix composite using top loaded bottom pouring stir casting method. Silicon [Internet]. 2023; 16:45-59.(0123456789). Available from: https://doi.org/10.1007/s12633-023-02648-4
9. Singh NK, Balaguru S, Rathore RK, Namdeo AK. Multi-criteria decision-making technique for optimal material selection of AA7075/SiC composite foam using COPRAS technique. 2023; 71(10):0-5. https://doi.org/10.18311/jmmf/2023/34005
10. Singh NK, Sethuraman B. Development and characterisation of Aluminium AA7075 Hybrid Composite Foams (AHCFs) using SiC and TiB2 reinforcement. Int J Met [Internet]. 2023. https://doi.org/10.21203/rs.3.rs-1718478/v1
11. Singh NK. Study of mechanical property of sintered iron preform. Int J Res Appl Sci Eng Technol. 2018; 6(2):351-4. https://doi.org/10.22214/ijraset.2018.2050
12. Parveez B, Jamal NA, Anuar H, Ahmad Y, Aabid A, Baig M. Microstructure and mechanical properties of metal foams fabricated via melt foaming and powder metallurgy technique: A review. Materials (Basel). 2022; 15(15):5302. https://doi.org/10.3390/ma15155302 PMid:35955234 PMCid: PMC9369530.
13. Verma KS, Muchhala D, Panthi SK, Mondal DP. Influences of cell size, cell wall thickness and cell circularity on the compressive responses of closed-cell aluminium foam and its FEA analysis. Int J Met [Internet]. 2021. https://doi.org/10.1007/s40962-021-00627-2
14. Muchhala D, Yadav BN, Kumar R, Mondal DP, Venkat ANC. Effect of SWCNTs content and relative density on the energy absorption capabilities of closed-cell Al-cenosphere-SWCNTs hybrid foam. Compos Part B Eng [Internet]. 2019; 176:107304. https://doi.org/10.1016/j.compositesb.2019.107304.
15. Birla S, Mondal DP, Das S, Khare A, Singh JP. Effect of cenosphere particle size and relative density on the compressive deformation behaviour of aluminium-cenosphere hybrid foam. Mater Des [Internet]. 2017; 117:168-77. https://doi.org/10.1016/j.matdes.2016.12.078
16. Sahu S, Barnwal AK, Mondal DP, Jain P. ZA27-SiCp composite foam through liquid metallurgy technique using CaH2 as a foaming agent ZA27-SiCp composite foam through liquid metallurgy technique using CaH2 as a foaming agent. 2013; 59(8):23-9. Available from: https://www.researchgate.net/publication/303792249